

## Electronic hyperpolarizability calculation without the periodic images error for a large nonlinear molecule

Y. Takimoto,<sup>1</sup> M. Otani,<sup>2</sup> and O. Sugino<sup>1</sup><sup>1</sup>*Institute for Solid State Physics, University of Tokyo, Kashiwa, Chiba 277-8581, Japan*<sup>2</sup>*National Institute of Advanced Industrial Science and Technology, Umezono 1-1-1, Tsukuba 305-8568, Japan*

(Received 15 January 2010; published 14 April 2010)

A Green's-function technique, i.e., the effective screening medium method of Otani and Sugino [Phys. Rev. B **73**, 115407 (2006)] for solving the Poisson's equation for a large organic nonlinear optical (NLO) molecule is investigated. This approach is essentially as efficient as the periodic treatment of the reciprocal-space method using fast Fourier transform while the direction along the dipole moment solved analytically under a given boundary condition. Unlike other correction methods such as the cutoff or multipole method, this scheme only requires the minimum size of the supercell. Here we study an application to the linear and second-order nonlinear optical properties of the NLO molecules in gas phase within the time-dependent density-functional theory and address a large periodic image error associated with the reciprocal-space method. We conclude that the Green's-function method is especially important and useful for a large-scale nonlinear molecule including future possibility of incorporating solvent effects.

DOI: [10.1103/PhysRevB.81.153405](https://doi.org/10.1103/PhysRevB.81.153405)

PACS number(s): 42.70.Mp, 31.15.E-, 42.70.Nq, 42.65.-k

Organic nonlinear optical (NLO) materials have gained popularity in recent years because of their prominent second- and third-order hyperpolarizability coefficients compared with those of inorganic NLO materials.<sup>1</sup> The material with large hyperpolarizabilities is important for optical telecommunication and photonic applications which require fast electrical-to-optical conversion and efficient optical modulation. One of the best organic NLO molecules consists of the electron donor-acceptor-substituted  $\pi$ -conjugated "push-pull" chromophore, which is known to cause large second hyperpolarizabilities.<sup>2</sup> In this context, the organic chromophores have become the target of theoretical studies. To help designing NLO devices, the dynamical properties need to be determined since the devices usually operate at a certain frequency or a band of frequencies. As the size of the NLO molecule of interest is normally large, the density-functional theory (DFT) based calculation of the gas phase molecule is a natural choice for the first theoretical study although incorporating intermolecular interactions and the solvent effects should be the target of future study. Such DFT calculations are, however, bottlenecked by the solution of the Poisson's equation; hence, the equation is often solved in reciprocal space using the fast Fourier transform (FFT). In such a calculation scheme, the large dipole moment of the NLO molecules causes serious periodic error.

The periodic error appears whenever the periodic boundary condition (PBC) is applied in the nonperiodic, e.g., isolated degrees of freedom, and has long been known in many different fields. This was the case in the previous study of one of the authors.<sup>3</sup> They have developed the real-time time-dependent density-functional theory (TDDFT) scheme to compute the linear and nonlinear dynamic hyperpolarizabilities for NLO molecules and studied the molecules by applying the three-dimensional PBC, whereby the Poisson's equation was solved efficiently using the FFT in reciprocal space. The second-order hyperpolarizability component obtained therein is found to contain significant periodic error, as it will be discussed in detail below. The error cannot be easily removed by enlarging the computational cell because of the

long-ranged dipole interaction. Therefore, it is essential for our purpose to use a Poisson's solver free from the periodic error and, most favorably, the solver of maximal efficiency because the target molecule is large.

Several different approaches have been proposed to solve the periodic error problem. The dipole correction<sup>4,5</sup> has been widely used, for example, in the first-principles calculation of surfaces, works for a static problem but cannot be easily used for a dynamical problem. The Coulomb cut-off method is another well-known method, whose performance on the application to dynamical problems was recently investigated by Rozzi *et al.*<sup>6</sup> The method requires, in the nonperiodic direction, the cell twice as large as that of the "minimal" cell or the cell just enough to contain the whole electron density. Such additional vacuum region may not be necessary if one explicitly solves the Poisson's equation under the correct boundary condition instead of using a correction scheme. In this regard, we focus on the technique developed by Otani and Sugino,<sup>7</sup> where the Green's function is handled without sacrificing the computational efficiency.

The Green's-function technique of Otani and Sugino was originally developed to describe a biased surface/interface slab by sandwiching it between two effective screening media (ESM) of permittivity. When one takes a planar boundary for the ESM, the Poisson's equation is quasi-one-dimensional in the surface normal direction, where the Green's function is analytically obtained and is easily handled. The computational cost thereby remains almost the same as that for the conventional FFT-based method when taking the cell of the same size. Numerical advantage for a large-scale surface calculation was discussed recently.<sup>8</sup>

In this Brief Report, we show that this ESM method is also useful for the hyperpolarizability calculation of the NLO molecules with a large dipole moment. Herein the ESM of permittivity one, or the vacuum, is used to sandwich the slab of NLO molecules whose largest dipole moment ( $z$ ) is directed normally toward the ESM. This modeling is adequate for our purpose because the  $z$  component of the of the second-order hyperpolarizability, i.e.,  $\beta_{zzz}$  or the vector aver-

age  $\beta_{\parallel}$  defined later, is much larger (typically more than an order of magnitude) and much more important than the other components for the device applications. Then, the Green's function is solved with an open boundary condition,<sup>8</sup> here after, we call this the "vacuum" condition (VAC). The results will be compared with those calculated by the conventional FFT method under the PBC, which shows how seriously the periodic error affects the calculation. The fact that the dynamic hyperpolarizabilities are obtained using the minimal cell is the important advantage of using the ESM, but more importantly, the scheme may also be extended to include the solvent effect because the ESM was originally invented for that purpose and was used for the metal/water interfaces.<sup>9</sup>

We computed static polarizability using the ground state DFT and dynamic hyperpolarizability coefficients using the TDDFT response theory. All the calculations were done using the electronic structure program SIESTA,<sup>10</sup> where the ESM method was implemented. The methods were applied to small molecules, CO, as well as the benchmark NLO molecule, *para*-Nitroaniline (pNA). We also calculated a large NLO chromophore, i.e., 2-[3-Cyano-4-(2-5-[2-(4-diethylamino-phenyl)-vinyl]-thiophen-2-yl-vinyl)-5,5-dimethyl-5H-furan-2-ylidene]-malononitrile (FTC) that we have previously studied. Atomic units (a.u.) are used unless otherwise stated. We use the convention B of Ref. 11 for the first hyperpolarizability  $\beta$ .

The electronic properties were calculated by using finite field perturbation theory by means of numerical differentiation with respect to a finite external electric field. The field strengths used were (in a.u.) 0.000,  $\pm 0.001$ , and  $\pm 0.002$ . The induced dipole moments were fit to a fourth-order polynomial to obtain the polarizabilities and hyperpolarizabilities. For the electronic polarizability calculation, the basis set must be extended from the default double  $\zeta$  with single polarization (DZP) basis set available in SIESTA. We have used total of five  $\zeta$  and four polarization (SZ4P) functions to add diffuseness and flexibility to the basis set for the first hyperpolarizabilities calculations. All atomic basis set uses Troullier-Martins generalized gradient approximation (GGA) pseudopotentials<sup>12</sup> and the Perdew-Burke-Ernzerhof (PBE) exchange-correlation functional.<sup>13</sup> A detailed description of the TDDFT method is available in Ref. 3.

We report the vector average of  $\beta_{ijk}$  given by

$$\beta_{\parallel} = \frac{1}{5} \sum_i (\beta_{iiz} + \beta_{izi} + \beta_{zii}), \quad (1)$$

with  $z$  axis defined by the direction of the dipole. The value  $\beta_{\parallel}$  is related to the EFISH experiment that measures the quantity  $\Gamma$  define by<sup>14</sup>

$$\Gamma = \gamma + \frac{\mu_0 \beta_{\parallel}}{3kT}, \quad (2)$$

where  $\gamma$  is a scalar measure of the second hyperpolarizability,  $\mu_0$  is the magnitude of the permanent dipole moment, and  $kT$  is the thermal energy.

For C-O bond length, the experimental value for the gas-phase  $r_{C-O} = 1.13$  Å is used. For the pNA molecule, we have used the optimized structure using the B3LYP functional<sup>15,16</sup>

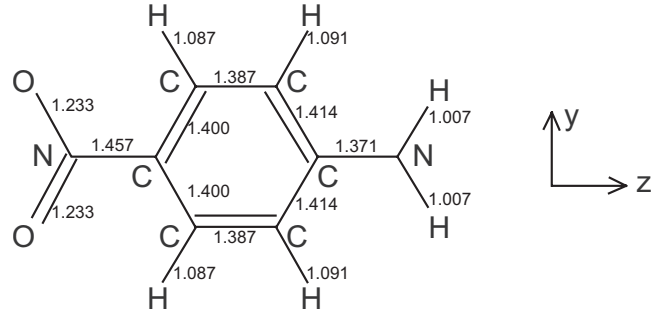


FIG. 1. The molecular structure of *p*-nitroaniline (pNA). The bond lengths are shown in Å.

obtained with aug-cc-pVDZ basis as illustrated in Fig. 1, confirmed that this provides sufficiently good agreement with the experimental geometry.<sup>17</sup> For the chromophore, we have chosen one particular conformer of the so-called FTC chromophores, which were developed by the Dalton group<sup>18</sup> and are currently used as a benchmarking molecule for NLO applications, because of high thermal and photochemical stability as well as an exceptionally large hyperpolarizability (Fig. 2). The geometry was optimized with the DFT code DMOL3 using the PBE functional and double numerical basis set with polarization functions in DMOL (DNP) numerical basis set.<sup>19</sup> The cut-off radius  $r_c$  is determined by requiring the energy shift  $\delta\epsilon$  to be less than  $0.5 \times 10^{-5}$  hartree for CO and pNA, and  $0.5 \times 10^{-6}$  hartree for FTC. The corresponding cut-off radius of the first- $\zeta$  orbitals with the energy shift  $0.5 \times 10^{-5}$  hartree are  $r_c^s(C) = 9.33$ ,  $r_c^p(C) = 12.91$ ,  $r_c^s(O) = 7.17$ ,  $r_c^p(O) = 9.93$ ,  $r_c^s(H) = 12.18$ , and  $r_c^s(N) = 8.00$ ,  $r_c^p(N) = 11.35$ , where  $r_c^s$  and  $r_c^p$  are the cut-off radius for atomic  $s$ -orbital and  $p$ -orbital, respectively. Similarly for the energy shift  $0.5 \times 10^{-5}$  hartree are  $r_c^s(C) = 8.03$ ,  $r_c^p(C) = 11.11$ ,  $r_c^s(O) = 6.33$ ,  $r_c^p(O) = 8.55$ ,  $r_c^s(H) = 10.48$ ,  $r_c^s(N) = 7.06$ ,  $r_c^p(N) = 9.53$ , and  $r_c^s(S) = 7.79$ ,  $r_c^p(S) = 10.51$ . We use the mesh cutoff size of 100 hartree for CO and pNA and 60 hartree for FTC.

Table I summarizes the results of static hyperpolarizabilities of CO, pNA, and FTC. For pNA and FTC, the first dynamic hyperpolarizability of the optical rectification (OR),  $\beta_{\parallel}(0; -\omega, \omega)$ , and the second harmonic generation (SHG),  $\beta_{\parallel}(-2\omega; \omega, \omega)$ , at 0.65 and 1.17 eV, respectively, are also calculated.

Results for the smallest molecule CO have the smallest dependence on the cell size and no significant difference between PBC and VAC. In particular, the first hyperpolarizability along the dipole direction  $\beta_{zzz}$  reduces by only a few percent as the cell size increases from the minimum cell,

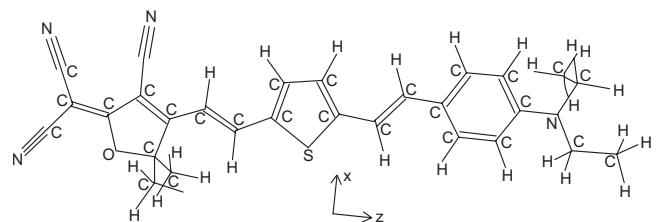


FIG. 2. Molecular structure of a representative conformer of the FTC chromophore.

TABLE I. Comparison of static polarizabilities and hyperpolarizabilities of CO, pNA, and FTC. The results are in the atomic unit (a.u.) unless otherwise specified. In all cases, the permanent dipole moment is along  $z$  axis. The third and fourth rows are the  $X$ ,  $Y$ , and  $Z$  value of the cell size being used.

	CO				pNA				FTC			
	PBC	PBC	PBC	VAC	PBC	PBC	PBC	VAC	PBC	PBC	PBC	VAC
$X \times Y$ (Å)	15 × 15				15 × 19				23 × 17			
$Z$ (Å)	15	45	120	15	20	60	200	20	36	108	216	36
$\mu$ (D)	0.247	0.246	0.246	0.245	7.840	7.553	7.458	7.419	26.18	22.61	21.89	21.17
$\alpha_{zz}$	15.4	15.4	15.3	15.3	173	166	164	162	1810	1510	1450	1400
$\bar{\alpha}$	13.2	13.1	13.1	13.1	111	109	108	108	837	735	716	697
$\beta_{zzz}$	14.3	14.0	13.9	13.8	951	822	783	766	40700	21900	18900	16100
$\beta_{xxz}$	4.18	4.15	4.14	4.13	-36.7	-38.5	-39.0	-39.2	3185	1860	1630	1420
$\beta_{yyz}$	4.18	4.15	4.14	4.13	-69.1	-68.2	-67.7	-67.7	-85	-99	-102	-103
$\beta_{\parallel}$	13.6	13.4	13.3	13.3	507	429	406	395	26300	14200	12200	10500
$\omega=0.65$ eV												
$\beta_{\parallel}(0; -\omega, \omega)$					556				434			
$\beta_{\parallel}(-2\omega; \omega, \omega)$					655				509			
$\omega=1.17$ eV												
$\beta_{\parallel}(0; -\omega, \omega)$					657				515			
$\beta_{\parallel}(-2\omega; \omega, \omega)$					1100				904			
$\beta_{\parallel}(-2\omega; \omega, \omega)$									1072 ± 44 <sup>a</sup>			

<sup>a</sup>The gas phase experimental result from Ref. 14.

which was determined by investigating the convergence behavior for VAC. The results are similar to each other presumably because of the fact that the required minimum cell size ( $15 \times 15 \times 15$ ) is rather large for this bimolecular system; it is required to obtain converged hyperpolarizabilities when extended basis is used. While, for the larger molecules, pNA and FTC, the value decreases by about 25% and 150%, respectively. It is noteworthy that the cell size required to match the VAC value for two digits is more than ten times larger than the minimum cell.

We had previously computed  $\beta$  for NLO molecules<sup>3,20</sup> with DZP basis set and PBC with the minimum cell. Although the result on pNA molecule was found to be close to the experimental gas phase value,<sup>14</sup> it was larger than the other theoretical calculation using the cluster model<sup>21</sup> which used the same PBE functional. The cell size affected our previous PBC calculation and the deviation can be mainly explained by the large cell size dependence; the basis set also affected the results but the amount is only a few percent which is significantly smaller than the cell size dependence.

Figures 3 and 4 are the UV absorption spectra computed with TDDFT using PBC and VAC with the smallest sized cell. The lowest absorption peak is characterized by the excitation of the charge transfer state. For pNA, the peak is located at 3.51 eV for PBC and 3.59 eV for VAC; and for FTC, it is located at 1.86 eV for PBC and 2.01 eV for VAC. In either case PBC absorptions are redshifted, 0.08 eV for pNA and 0.15 eV for FTC, because of the interaction with periodic images. Note that 0.15 eV shift in the linear absorption for FTC causes about 0.3 eV shift in the first resonant peak in the SHG nonlinear effect.

Figure 5 illustrates the Coulomb potential averaged over  $x$  and  $y$  directions. It is clear from this figure that the potential of PBC has a slope in the vacuum region, indicating that external field is virtually applied to the FTC molecule. This is an artifact of the PBC calculation. The effect still exists for the largest cell,  $23 \times 17 \times 216$ , six times larger than the smallest one. The potential looks gradually converge to the curve obtained with VAC. This shows efficiency of the ESM method for which the slope is naturally removed without any correction scheme.

In this Brief Report, the periodic image error in the electronic hyperpolarizabilities calculation was investigated. With the ESM method that uses the Green's function of correct boundary condition, we can efficiently remove the error in the direction along the permanent dipole. We compared

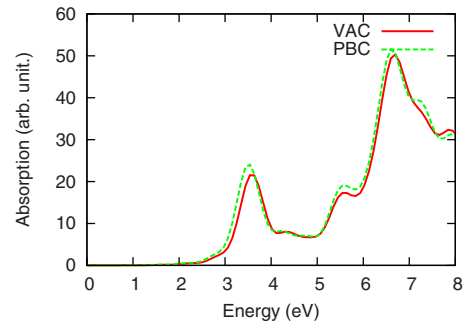


FIG. 3. (Color online) pNA UV absorption spectra using TD-DFT with two different boundary condition for solving the Hartree potential. Exponential broadening of 0.3 eV is included.

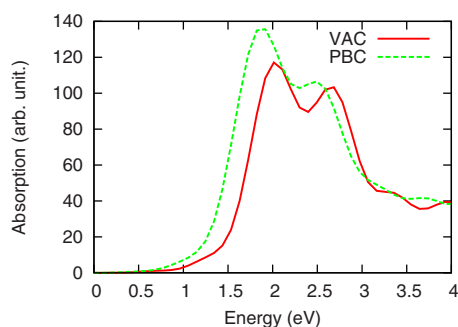


FIG. 4. (Color online) FTC UV absorption spectra. Exponential broadening of 0.3 eV is included.

the results obtained with the ESM with those obtained with PBC of various cell sizes and showed that the PBC result very slowly converges to the ESM result because of the long-ranged dipole interaction. The cell size required to achieve the convergence is about an order of magnitude larger than the minimum cell or the cell required for the ESM calculation. The result indicates that PBC is quite incapable for simulating nonlinear properties of NLO molecules whereas it has been widely used for solving the Poisson's equation or obtaining the Hartree potential because of simplicity and scalability. Indeed, use of the minimum cell for PBC calculation leads to overestimation of the first hyperpolarizability  $\beta_{zzz}$  by a factor of 2.5 in case of the FTC chromophore. The periodic image error affects also the shift of the peak location as well as the oscillator strength in the linear absorption, which further affects the value of hyperpolarizabilities.

The advantage of the ESM method thus consists in the efficiency, i.e., requirement of only the minimum size of supercell, and the accuracy, i.e., use of correct boundary condition for the Poisson's solver. Another advantage is that it is

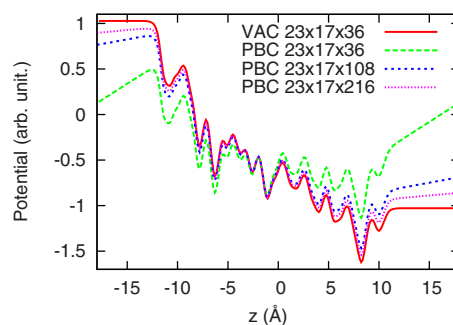


FIG. 5. (Color online) FTC Hartree potential illustrated along the direction of permanent dipole averaged over the other directions. Three different cell sizes are used for the periodic boundary condition by increasing the size of cell in the dipole direction.

capable of treating various boundary conditions, i.e., not only vacuum but also metallic as well as dielectric medium. When choosing the dielectric medium, the calculation is equivalent to using the polarizable continuum model (PCM) (Ref. 22) of a planar shape. Although the ESM was originally developed for the slab configuration, similar methods were recently developed to treat nonplanar configurations.<sup>23–26</sup> This suggests a future possibility of incorporating the solvent effects into the nonlinear study.

This work was partially supported by New Energy and Industrial Technology Development Organization (NEDO) and Next Generation Supercomputer Project of the Ministry of Education, Culture, Sports, Science and Technology (MEXT). Numerical calculations were performed at the Supercomputer Center, Institute for Solid State Physics, University of Tokyo.

<sup>1</sup>A. Mahapatra and E. Murphy, *Optical Fiber Telecommunications IVA* (Academic Press, San Diego, 2002), pp. 258–294.

<sup>2</sup>S. R. Marder, *Chem. Commun. (Cambridge)* **2006**, 131.

<sup>3</sup>Y. Takimoto, F. D. Vila, and J. J. Rehr, *J. Chem. Phys.* **127**, 154114 (2007).

<sup>4</sup>J. Neugebauer and M. Scheffler, *Phys. Rev. B* **46**, 16067 (1992).

<sup>5</sup>L. Bengtsson, *Phys. Rev. B* **59**, 12301 (1999).

<sup>6</sup>C. A. Rozzi, D. Varsano, A. Marini, E. K. U. Gross, and A. Rubio, *Phys. Rev. B* **73**, 205119 (2006).

<sup>7</sup>M. Otani and O. Sugino, *Phys. Rev. B* **73**, 115407 (2006).

<sup>8</sup>I. Hamada, M. Otani, O. Sugino, and Y. Morikawa, *Phys. Rev. B* **80**, 165411 (2009).

<sup>9</sup>M. Otani, I. Hamada, O. Sugino, Y. Morikawa, Y. Okamoto, and T. Ikeshoji, *J. Phys. Soc. Jpn.* **77**, 024802 (2008).

<sup>10</sup>J. M. Soler, E. Artacho, J. D. Gale, A. García, J. Junquera, P. Ordejón, and D. Sánchez-Portal, *J. Phys.: Condens. Matter* **14**, 2745 (2002).

<sup>11</sup>A. Willetts, J. E. Rice, D. M. Burland, and D. P. Shelton, *J. Chem. Phys.* **97**, 7590 (1992).

<sup>12</sup>N. Troullier and J. L. Martins, *Phys. Rev. B* **43**, 3993 (1991).

<sup>13</sup>J. P. Perdew, K. Burke, and M. Ernzerhof, *Phys. Rev. Lett.* **77**, 3865 (1996).

<sup>14</sup>P. Kaatz, E. A. Donley, and D. P. Shelton, *J. Chem. Phys.* **108**,

849 (1998).

<sup>15</sup>A. D. Becke, *J. Chem. Phys.* **98**, 5648 (1993).

<sup>16</sup>P. Stephens, F. Devlin, C. Chabalowski, and M. Frisch, *J. Phys. Chem.* **98**, 11623 (1994).

<sup>17</sup>F. Sim, S. Chin, M. Dupuis, and J. E. Rice, *J. Phys. Chem.* **97**, 1158 (1993).

<sup>18</sup>L. Dalton, A. Harper, A. Ren, F. Wang, G. Todorova, J. Chen, C. Zhang, and M. Lee, *Ind. Eng. Chem. Res.* **38**, 8 (1999).

<sup>19</sup>Materials Studio and DMol3; Accelrys: San Diego, 2002.

<sup>20</sup>Conversion factor from the previous paper is following:  $\beta$  1 au =  $8.6392 \times 10^{-33}$  esu, and  $\beta_{||} = \frac{3}{5}\beta_z$ ; i.e., multiply by 69.45 to obtain  $\beta_{||}$  in a.u. from the previous results.

<sup>21</sup>J. R. Hammond and K. Kowalski, *J. Chem. Phys.* **130**, 194108 (2009).

<sup>22</sup>J. Tomasi and M. Persico, *Chem. Rev.* **94**, 2027 (1994).

<sup>23</sup>J.-L. Fattebert and F. Gygi, *Int. J. Quantum Chem.* **93**, 139 (2003).

<sup>24</sup>D. A. Scherlis, J.-L. Fattebert, F. Gygi, M. Cococcioni, and N. Marzari, *J. Chem. Phys.* **124**, 074103 (2006).

<sup>25</sup>R. Jinnouchi and A. B. Anderson, *Phys. Rev. B* **77**, 245417 (2008).

<sup>26</sup>H.-F. Wang and Z.-P. Liu, *J. Phys. Chem. C* **113**, 17502 (2009).